Figure S1. Characterization of the HECTD1-KD cells in the HeLa cell line. (A) KD of HECTD1 in HeLa cells was established through the stable transfection of shRNA or scrambled shRNA, known as the Ctrl. Expression levels of HECTD1 were assessed by western blot analysis using an anti-HECTD1 antibody. (B) Proliferation of HeLa Ctrl and HECTD1-KD cells in the presence/absence of 100 ng/ml epidermal growth factor treatment was determined using a cell proliferation assay. Absorbance at 490 nm was measured at 0, 30, 48 and 72 h following seeding and absorbance was normalized to the absorbance at 0 h. shRNA, short hairpin RNA; Ctrl, negative control; HECTD1, HECT domain E3 ubiquitin ligase 1.

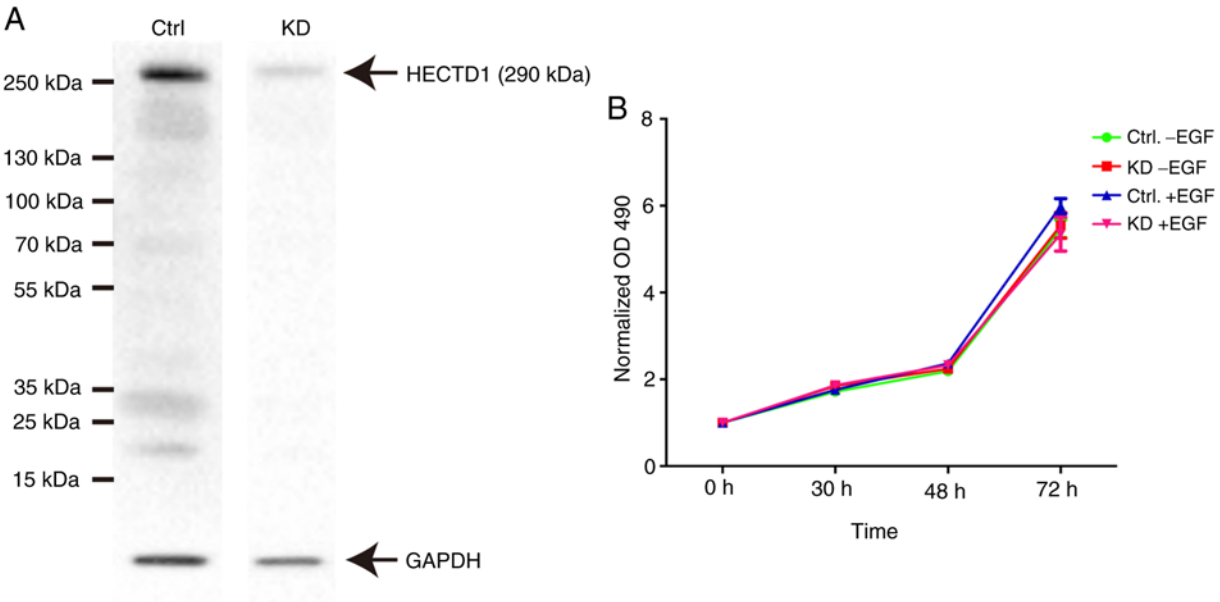

Figure S2. SNAIL protein stability was examined using the cycloheximide chase assay in Ctrl and HECTD1-KD cells and western blot analysis was performed. SNAIL expression levels gradually increased following 12 h in HECTD1-KD cells. HECTD1, HECT domain E3 ubiquitin ligase 1; KD, knock-down; Ctrl, negative control.

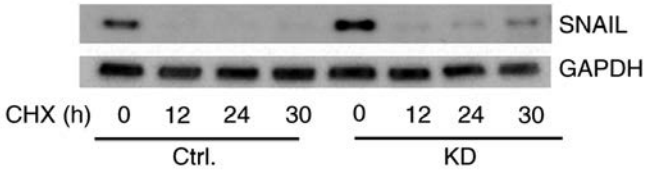

Figure S3. Prediction of NLS and NES in HECTD1. (A) Prediction of NLS ins HECTD1 was carried out using two databases: (a) www.moseslab.csb.utoronto.ca/NLStradamus/ and (b) http://nls-mapper.iab.keio.ac.jp/cgi-bin/NLS_Mapper_y.cgi. (B) Prediction of NES of HECTD1 using NetNES 1.1 Server (www.cbs.dtu.dk/services/NetNES). (C) Prediction of subcellular localization of HECTD1 using two databases: (a) http://crdd.osdd.net/cgibin/rslpred/chkres?7160 and (b) PSORT (*https://psort.hgc.jp*). NLS, nuclear localization signals; NES, nuclear export signals; HECTD1, HECT domain E3 ubiquitin ligase 1.

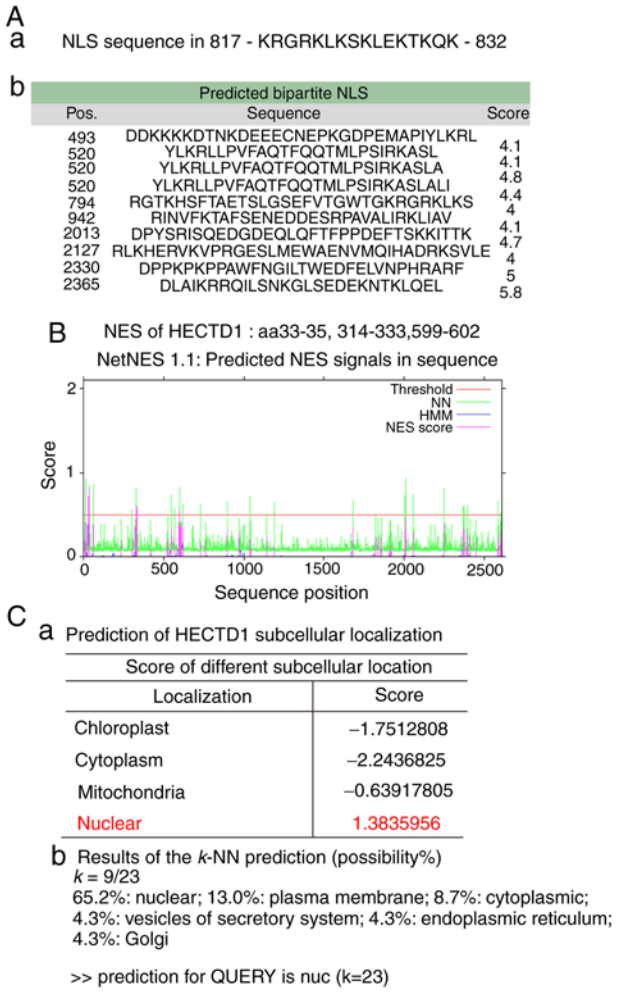

Figure S4. Relative protein expression in control (Ctrl, scrambled shRNA transfected) and HECTD1 knockdown (KD) cells upon stimulation with EGF with time (min). (A) SNAIL Ctrl, SLUG Ctrl, VIM Ctrl, E-Cad and N-Cad Ctrl indicate the relative expression of SNAIL, SLUG, VIM, E-Cad and N-Cad in control cells; SNAIL KD, SLUG KD, VIM KD, E-Cad KD and N-Cad KD represent the relative expression of SNAIL, SLUG, VIM, E-Cad and N-Cad in KD cells. (B) Relative expression of total ERK1/2 in Ctrl and KD cells.

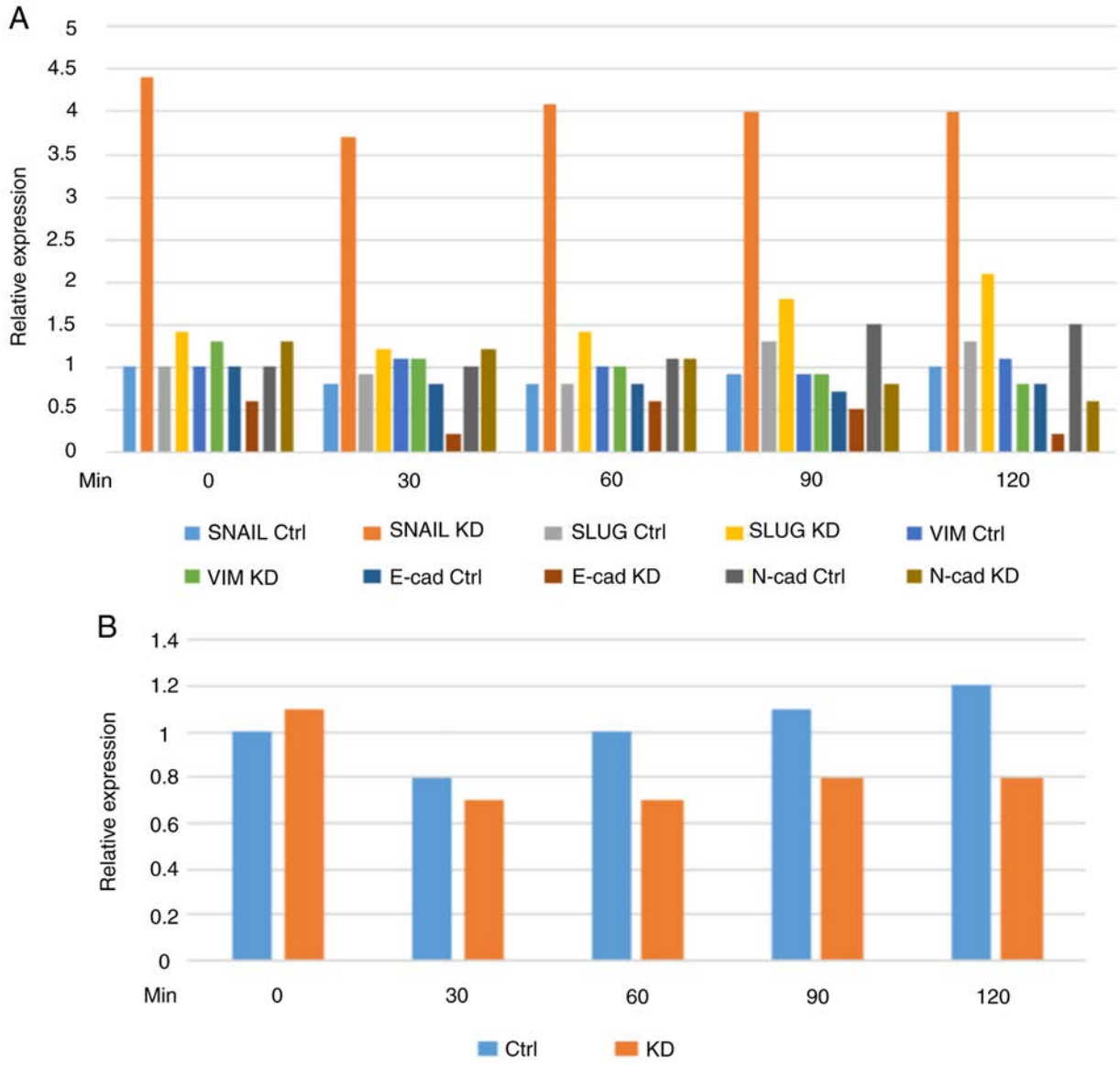

Figure S5. Tissue microarrays of tumor specimens from 4 patients with cervical cancer. Immunohistochemistry was performed using an anti HECTD1 antibody (middle panel) and an anti-SNAIL antibody (right panel). Case 1 presents the sample from patient ID 30, aged 39, with cervix, T-83000; squamous cell carcinoma; NOS, M-80703. Case 2 presents patient ID 978, aged 40; with cervix, T-83000; squamous cell carcinoma; NOS, M-80703; case 3 presents patient ID 1751; aged 34; with cervix, T-83000; squamous cell carcinoma; NOS, M-80703; and case 4 presents patient ID 2480; aged 44; with T-83000; adenocarcinoma; NOS, M-81403.

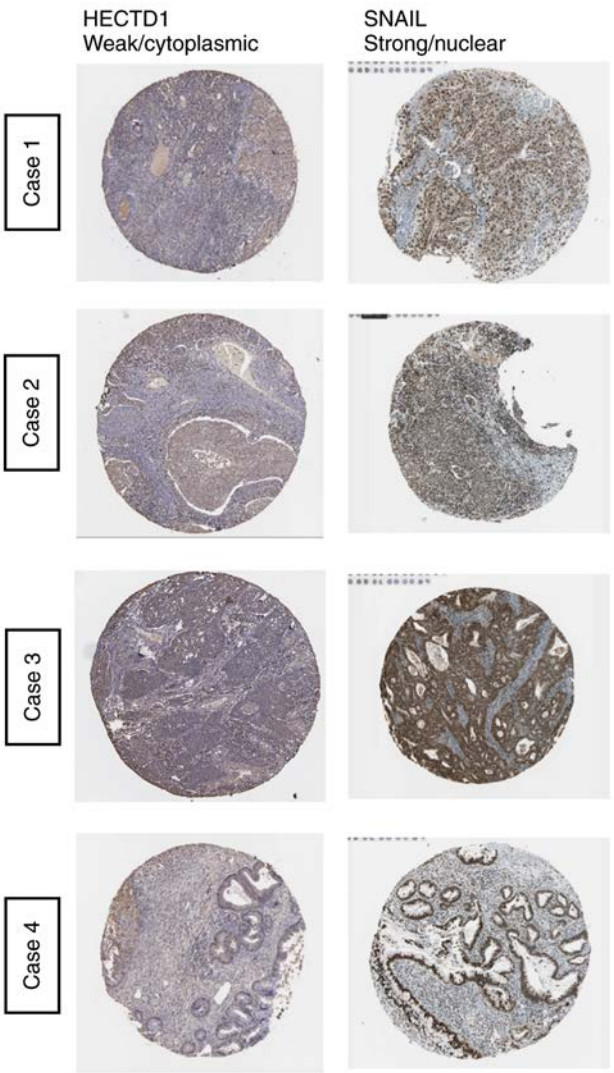

Figure S6. Kaplan-Meier plots of relapse-free patient survival vs. *HECTD1* expression levels in 6 types of cancer.

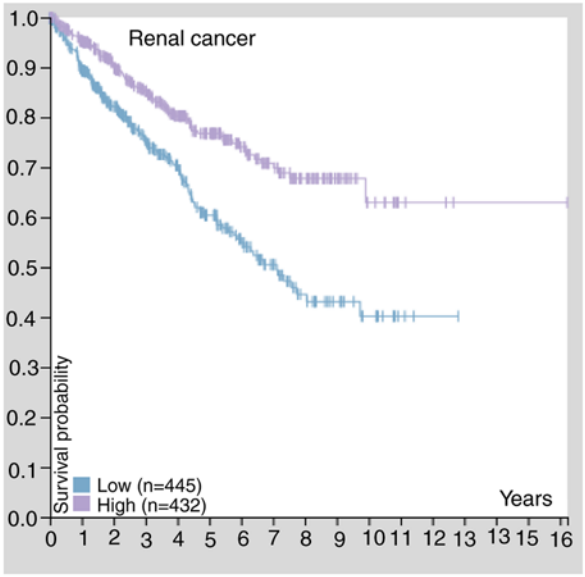

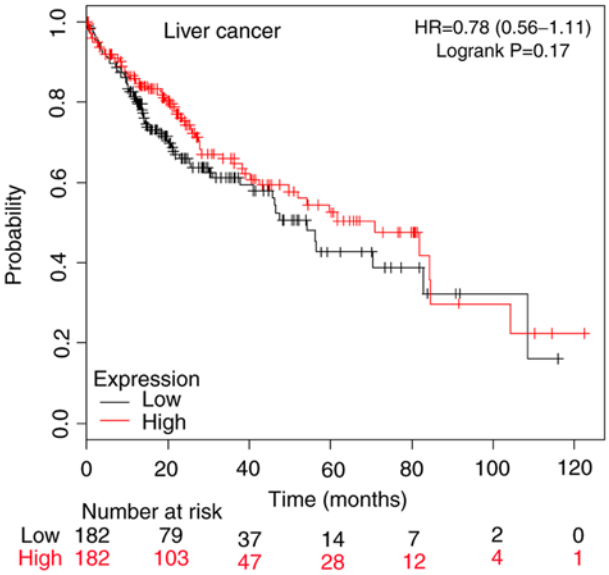

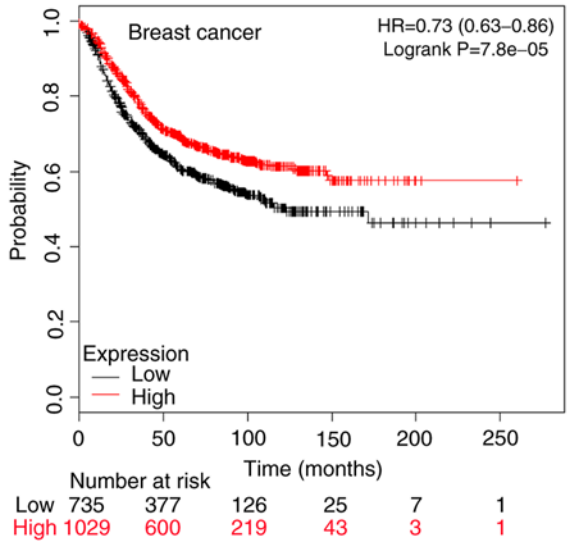

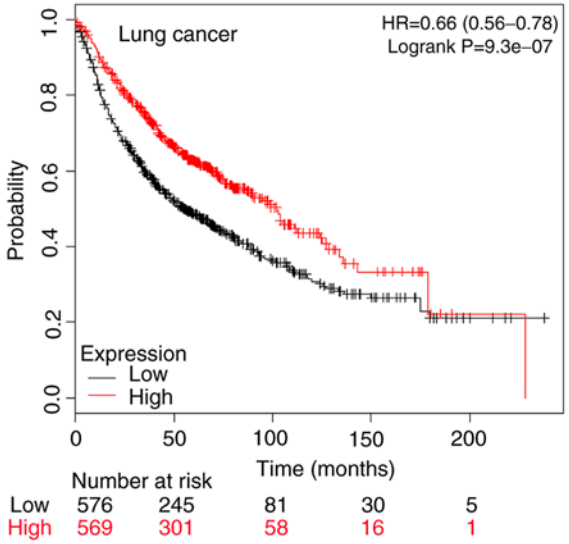

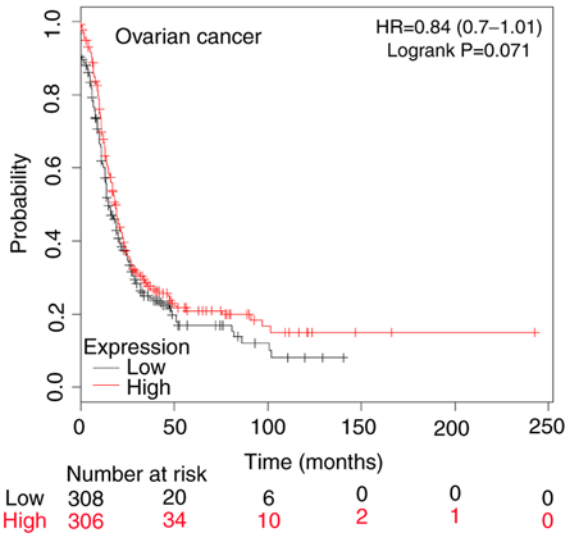

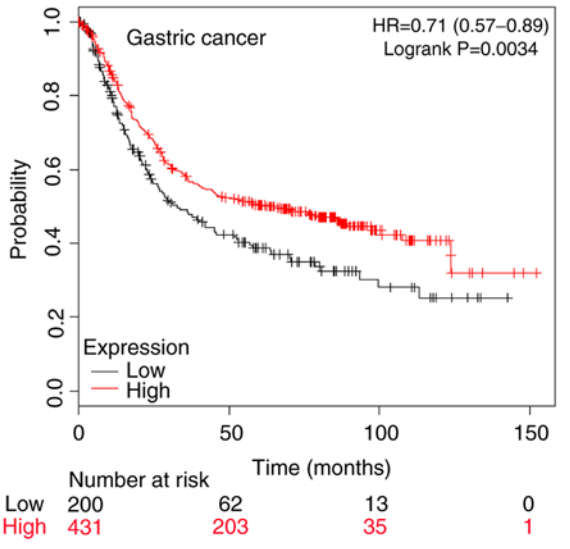

Figure S7. Kaplan-Meier plots of relapse-free patient survival vs. microRNA-210 expression levels in breast and liver cancer.

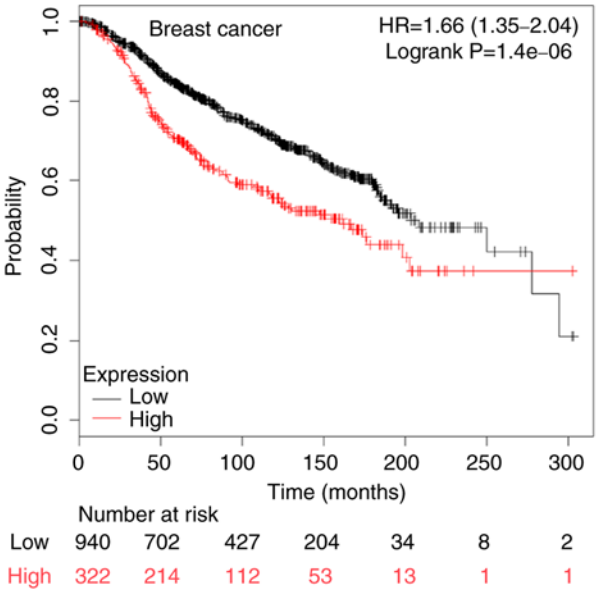

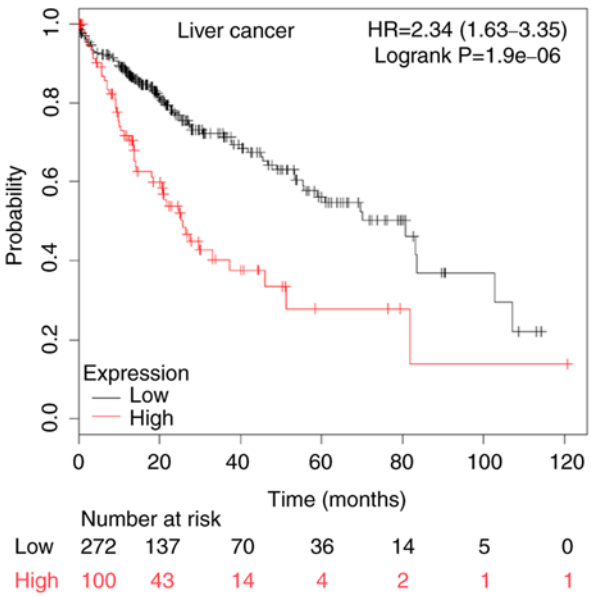

Table SI. Somatic mutations identified in the cervix and ovary.

Body part	Missense	Synonymous	Frameshift	Stop	Total
Cervix	20	3	1	0	24
Ovary	10	2	1	1	14

Table SII. Somatic mutations of HECTD1 in the cervix.

Mutations	Consequences
chr14:g.31109551G>A	Missense HECTD1 T2109M
chr14:g.31141877C>T	Missense HECTD1 E952K
chr14:g.31172090G>C	Missense HECTD1 Q397E
chr14:g.31128985C>T	Synonymous HECTD1 R1462R
chr14:g.31109515C>T	Missense HECTD1 G2121E
chr14:g.31141910C>G	Missense HECTD1 E941Q
chr14:g.31144861G>C	Synonymous HECTD1 L859L
chr14:g.31175002G>A	Missense HECTD1 S171L
chr14:g.31174976G>C	Missense HECTD1 Q180E
chr14:g.31149127C>T	Missense HECTD1 R730K
chr14:g.31127939delA	Frameshift HECTD1 M1610Cfs*12
chr14:g.31109439C>T	Synonymous HECTD1 E2146E
chr14:g.31136609C>G	Missense HECTD1 L1012F
chr14:g.31127969C>A	Missense HECTD1 L1599F
chr14:g.31114055C>T	Missense HECTD1 C1893Y
chr14:g.31109533A>G	Missense HECTD1 V2115A
chr14:g.31156909A>C	Missense HECTD1 I621M
chr14:g.31129403C>T	Missense HECTD1 R1323H
chr14:g.31149140C>T	Missense HECTD1 E726K
chr14:g.31119770C>G	Missense HECTD1 D1779H
chr14:g.31113294G>A	Missense HECTD1 S2016L
chr14:g.31101241G>A	Missense HECTD1 C2545Y
chr14:g.31112431C>T	Missense HECTD1 A2088V
chr14:g.31171910C>T	Missense HECTD1 S428L

Table SIII. Somatic mutations of HECTD1 in the ovary.

Mutations	Consequences
chr14:g.31114054G>C	Missense HECTD1 C1893W
chr14:g.31135567G>A	Stop Gained HECTD1 R1055*
chr14:g.31105407G>T	Missense HECTD1 Q2459K
chr14:g.31173694C>T	Missense HECTD1 R239Q
chr14:g.31100974G>A	Missense HECTD1 R2597C
chr14:g.31178247G>T	Missense HECTD1 P50T
chr14:g.31106892A>T	Missense HECTD1 F2327Y
chr14:g.31129126A>C	Missense HECTD1 S1415R
chr14:g.31119732A>C	Synonymous HECTD1 T1791T
chr14:g.31106985 DelT	Frameshift HECTD1 L2296fs*21
chr14:g.311139662 G>A	Missense HECTD1 A1923T
chr14:g.31109509 T>A	Missense HECTD1 F2123Y
chr14:g.31128960 C>T	Missense HECTD1 R1471C
chr14:g.31172082 A>T	Missense HECTD1 L399L